

# Coupling modes in high-frequency multiple scattering problems: the case of two circles

Daan Huybrechs  
 daan.huybrechs@cs.kuleuven.be  
 Department of Computer Science  
 KU Leuven, Belgium

Peter Opsomer (corresponding author)  
 peter.opsomer@cs.kuleuven.be  
 Department of Computer Science  
 KU Leuven, Belgium

October 25, 2018

## Abstract

One can reformulate a high-frequency scattering problem as a boundary integral equation. In the presence of multiple scattering obstacles, the wave pattern becomes very complicated, but wavenumber-independent simulation schemes have been proposed based on ray tracing. In such schemes, one can note that the phases of the corresponding densities on each of the obstacles converges to an equilibrium after a few iterations. For the case of two circular scatterers, we will compute a Taylor approximation of this limiting phase, independently of the incident wave and with a computational complexity independent of the wavenumber.

**Keywords:** Boundary Element Method, Oscillatory integration, High-frequency scattering, Multiple obstacles, Periodic orbits, Phase extraction.

**MSC:** Primary: 65N38, Secondary : 45A05, 45M05, 65R20.

## 1 Introduction

Numerical simulations in acoustics are often based on a Boundary Integral equation reformulation of the Helmholtz equation, see for example [10, 21]. An incoming wave that is scattered by an obstacle with boundary  $\Gamma$  results in a scattered field  $u^s(\mathbf{x})$  that can be represented by the so-called *single layer potential*,

$$u^s(\mathbf{x}) = (Sv)(\mathbf{x}) = \int_{\Gamma} K(\mathbf{x}, \mathbf{y}) v(\mathbf{y}) ds(\mathbf{y}). \quad (1)$$

Here,  $K(\mathbf{x}, \mathbf{y})$  is the Green's function of the Helmholtz equation with wavenumber  $k$  and  $v(\mathbf{y})$  is the unknown *density function*, defined on  $\Gamma$ . Though other representations of the scattered field exist, for the analysis in this paper, the equation above is the simplest to proceed with and sufficient to obtain the results.

So-called hybrid numerical-asymptotic methods aim to avoid refining the discretization for increasing  $k$  by incorporating information about the solution from asymptotic analysis (see the review [8] and references therein). In particular, phase-extraction methods use information about the phase  $g$  of the solution  $v(\mathbf{y})$  in order to discretize only the remaining non-oscillatory part  $f$  in the following factorization:

$$v(\mathbf{y}) = f(\mathbf{y}, k) e^{ikg(\mathbf{y})}. \quad (2)$$

Phase extraction methods are simplest for convex obstacles, and require ray-tracing or similar techniques for more complicated domains or multiple scattering configurations [7, 12, 11, 2, 13, 9, 3, 4, 1]. For an overview, see [5, 8].

Ray tracing methods for scattering configurations with multiple obstacles at high frequencies lead to a sequence of single-scattering problems, where the phase can be extracted in each case. The first computation

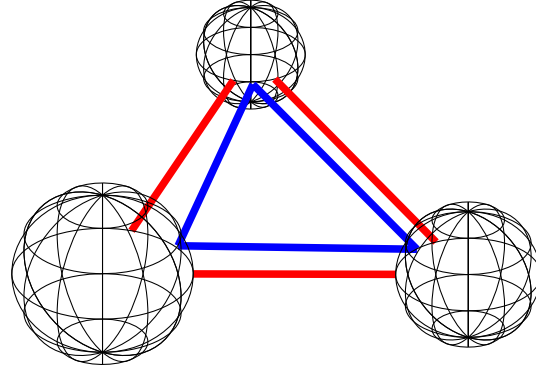


**Figure 1:** Depiction of periodic orbits between three spherical scatterers: one periodic orbit visits all three scatterers in a triangle-shaped trajectory minimizing the total path length (blue), and one periodic orbit exists between each combination of two spheres (red).

is the scattering of the incoming wave by just one of the obstacles. Next, the reflected field is considered as an incoming wave for another obstacle, and so on. This process is repeated and care has to be taken to include all reflections by all obstacles until convergence. It was shown by Ecevit et al. that the sequence of single-scattering problems can be organised according to certain *periodic orbits* [11, 2]. Examples of these are illustrated in Figure 1. Each such orbit consists of the shortest path between a subset of obstacles, and one can intuitively understand them as follows. Rays originate in a source and reflect off obstacles in the scene. Rays that do not reflect on another obstacle leave the scene forever. For rays that do, one can repeat the reasoning on the next iteration of reflections. Fewer and fewer rays will remain, and those that do are close to the aforementioned periodic orbits. Indeed, a ray that travels exactly *on* the shortest path between a collection of obstacles remains trapped in the scene forever, while any other ray ultimately leaves the scene.

Rays that travel along a periodic orbit induce a density on each of the participating obstacles. We will call the corresponding density a ‘mode’, and note that it has the same structure as (2):

$$V_j(\tau) \sim v_{j,\text{smooth}}(\tau) e^{ik\phi_j(\tau)}, \quad j = 1, \dots, J. \quad (3)$$

Here,  $J$  is the number of obstacles in the orbit. One can observe that the densities of rays travelling close to the periodic orbits converge to a limit. One can see this in for example [12, Fig. 1 & 2], although this feature was not further investigated there. We will aim to calculate the limiting phases, i.e. the functions  $\phi_j$  in the above expression.

The modes can be seen as eigenfunctions of the multiple scattering problem. Indeed, the existence of a limit indicates that a wave with the density  $V_1$  on the first obstacle induces a density  $V_2$  on the second obstacle,  $V_3$  on the third obstacle and so on, such that the last density  $V_J$  induces precisely the density  $V_1$  again on the first obstacle, up to a constant factor. This constant factor can be seen as an eigenvalue, and the collection of densities on each of the obstacles is an eigenfunction of the sequence of single scattering problems.

In our initial study, we restrict ourselves to the case of two circles, as shown in Figure 2. In this case, there is a single periodic orbit, namely the shortest path between the two circles. We analyze the limiting phase via its Taylor series around the point where the shortest path hits the boundary. Using symmetry, it is sufficient to study a single phase function. The advantage of the Taylor series approximation is that it leads to fully explicit expressions.

Our implementation of the numerical experiments in this paper is publicly available on GitHub [18] and a copy of the code can always be obtained from the authors.

## 2 Setting and problem statement

We formulate the problem as an eigenvalue problem for an oscillatory integral operator that represents scattering by a circle. Looking for eigenfunctions of the form (2) leads to oscillatory integrals. In order to analyze these asymptotically for a large wavenumber  $k$ , we use the well-known method of steepest descent [20, 6]. It deforms the path of integration into the path of steepest descent  $h(p)$  in the complex plane such that oscillating integrands are transformed to rapidly decaying integrands.

A similar methodology was employed in [14] to find the asymptotic expansion of the solution of a scattering problem, possibly involving multiple obstacles as well. In particular, the method of steepest descent was used in [14] to track the forward propagation of rays, given an initial incoming wave. The main difference is that in our current setting, we are concerned with an eigenvalue problem instead.

The non-overlapping circles in Figure 2 are separated by a distance  $d$  and the corresponding shortest path is the periodic orbit along which rays will be trapped forever. We parametrize the circles as

$$\begin{aligned}\Gamma_1(\tau) &= r[\sin(2\pi\tau), \cos(2\pi\tau)], \quad \tau \in [0, 1], \\ \Gamma_2(\tau) &= [0, d + 2r] + r[\sin(2\pi\tau), -\cos(2\pi\tau)], \quad \tau \in [0, 1],\end{aligned}$$

with  $r$  and  $d > 0$  such that  $\tau = 0$  gives the points on the circles closest to each other. The unknown phase function for the density on  $\Gamma_1$  is denoted  $\phi_1(\tau)$ . Due to symmetry, we have that  $\phi_2(\tau) = \phi_1(\pm\tau) + \nu$ , where  $\nu$  is a constant phase factor. We choose  $\phi_2(\tau) = \phi_1(\tau)$ .

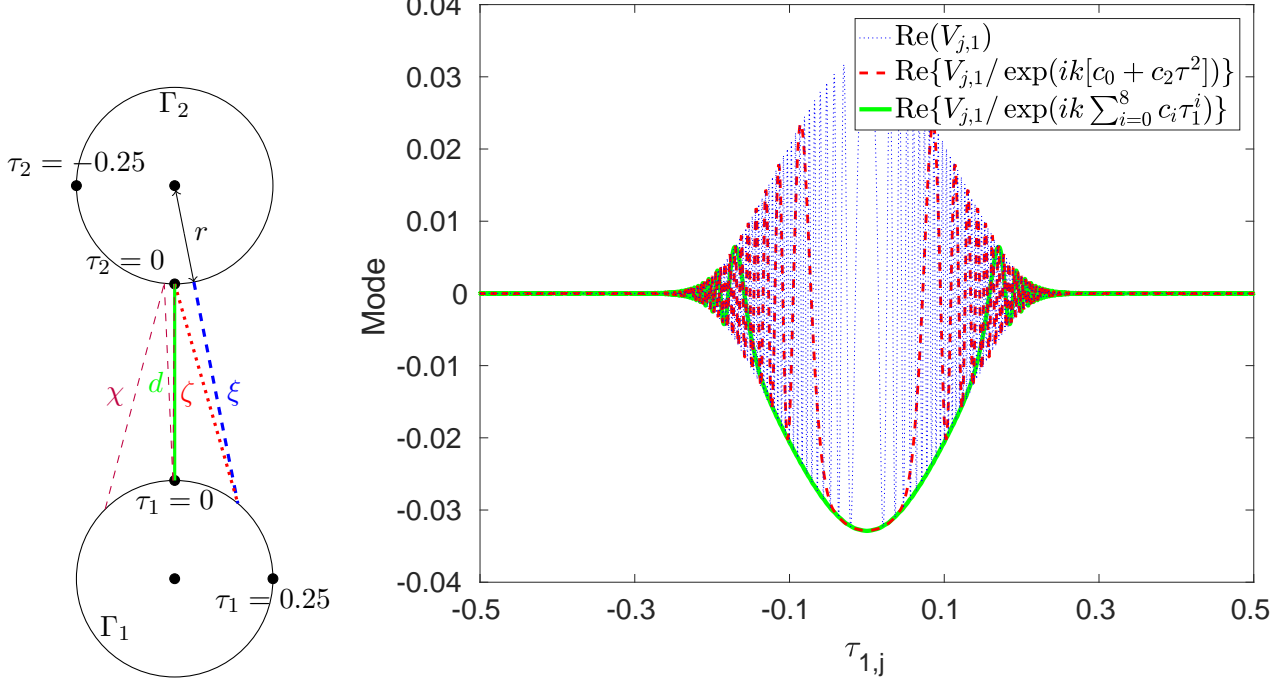


**Figure 2:** Two circles under consideration in this paper (left) and a numerical illustration of the eigenvector  $V_{j,1}$  of the discrete operator  $M$ , divided by different phases (right). The parameters are  $k = 2^9$ ,  $r = \frac{1}{2}$  and  $d = 1$ .

In order to formulate the eigenvalue problem, recall the single layer potential (1). We shall use the notation  $S_{ij}v_i$  for its application on a density  $v_i$  defined on  $\Gamma_i$ , and with the point  $\mathbf{x}$  on  $\Gamma_j$ . An incident wave on  $\Gamma_j$  is written as  $u_j^{\text{inc}}$ . Disregarding the possibility of resonances, for the time being, the single layer potential leads to coupled integral equations of the first kind for a multiple scattering sound-soft Dirichlet problem,

$$S_{11}v_1 + S_{21}v_2 = -u_1^{\text{inc}},$$

$$S_{12}v_1 + S_{22}v_2 = -u_2^{\text{inc}}.$$

The operator under investigation in this paper is given succinctly by

$$Tv = S_{11}^{-1}S_{21}S_{22}^{-1}S_{12}v, \quad (4)$$

and in particular, we look for a function  $v_1$  of the form (2) such that

$$Tv_1 = \lambda v_1.$$

A discretisation of the combined multiple scattering problem leads to a BEM matrix  $A$  with the following block structure form,

$$A = \begin{pmatrix} A_{11} & A_{21} \\ A_{12} & A_{22} \end{pmatrix}.$$

Here,  $A_{11}$  and  $A_{22}$  respectively represent the self-interaction of the first and second obstacle, while  $A_{21}$  gives the action of the density on  $\Gamma_2$  on the location of the first circle  $\Gamma_1$ . A full cycle of reflections is represented by

$$M = A_{11}^{-1}A_{21}A_{22}^{-1}A_{12} = VDV^{-1}.$$

The discrete operator  $M$  corresponds closely to  $T$  in (4).

In order to illustrate the coupling mode between two circles, we have used a collocation discretisation with piecewise linear approximation of the density function. In this case, the first eigenvector of  $M$  is the mode we are looking for, evaluated at the collocation points on  $\Gamma_1$ . It is shown in the right panel of Figure 2. This is an oscillatory function, but factoring out the Taylor approximation of  $\phi(\tau)$  (which we will compute later on) provides a much less oscillatory function. One can also note that it is supported in the region where the circles can ‘see’ each other. The corresponding highest eigenvalue  $D_{1,1}$  equals  $\lambda$ , and its phase is  $2d$ . The latter is the twice the distance between the circles in Figure 2, which is also the length of the periodic orbit studied in [11, 2] and here.

We proceed by analyzing the operator  $T$  asymptotically for large  $k$ . Due to symmetry, we only have to analyze  $S_{11}$  and  $S_{21}$ . We proceed with the latter first, since it does not appear with its inverse in (4).

### 3 Field scattered by the second circle onto the first circle

When we calculate the field that  $\Gamma_2$  scatters onto the location  $\Gamma_1$ , we obtain

$$\begin{aligned} u^s(\tau_1) &= S_{21}V_2 = \int_{\Gamma_2} \frac{i}{4} H_0^{(1)}(k\delta[\tau_1, \tau_2]) V_2(\tau_2) d\Gamma_2, \\ u^s(\tau_1) &\sim \int_0^1 \frac{i}{4} (k\delta[\tau_1, \tau_2]\pi/2)^{-1/2} e^{ik\delta[\tau_1, \tau_2] - i\pi/4} v_{2,\text{smooth}}(\tau_2) e^{ik\phi_2(\tau_2)} \|\nabla\Gamma_2(\tau_2)\|_2 d\tau_2, \end{aligned} \quad (5)$$

where  $\delta(\tau_1, \tau_2) = \|\Gamma_1(\tau_1) - \Gamma_2(\tau_2)\|_2$  is the Euclidean distance between two points on the circles. We have replaced the Hankel function  $H_0^{(1)}$  by the leading order term of its expansion for large arguments. More terms in the expansion can be found by substituting the full expansion, a process detailed in [14].

As is standard in asymptotic expansions of integrals [20, 15, 6], one notes that the only important contribution to an oscillatory integral originates in a region around the stationary point of the phase. This means finding a function  $\chi(\tau)$  such that

$$\left. \frac{\partial \delta[\tau_1, \tau_2] + \phi(\tau_2)}{\partial \tau_2} \right|_{\tau_2=\chi(\tau_1)} = 0. \quad (6)$$

The phase of the resulting integral (5) will then be  $\delta[\tau_1, \chi(\tau_1)] + \phi[\chi(\tau_1)]$ .

Physically, this means that the scattered field due to density  $V_2$  on  $\Gamma_2$  consists of rays, and that the ray hitting the point  $\tau_1$  on  $\Gamma_1$  comes from the point  $\chi(\tau_1)$  on  $\Gamma_2$ . In particular, we know that  $\chi(0) = 0$ , since that is precisely the periodic orbit, and we intend to study only local perturbations of this point.

## 4 Single scattering problem on the first circle

Next, we consider  $S_{11}^{-1}$ . A full computation of the asymptotic expansion of the solution to a single scattering problem, even with phase extraction, is rather involved. The computation is carried out in [14]. The problem of computing the phase of the solution is simpler since, in fact, it is known that the phase of the solution equals the phase of the incoming wave.

For completeness, the process of obtaining full asymptotics is as follows. Assuming a density of the form (3), the application of the integral operator on  $\Gamma_1$  yields

$$S_{11}V_1(\tau_1) = u(\tau_1) = \int_{\Gamma_1} \frac{i}{4} H_0^{(1)}(k\|\Gamma_1(\tau) - \Gamma_1(\tau_1)\|_2) \left( v_{1,\text{smooth}}(\tau) e^{ik\phi_1(\tau)} \right) \|\nabla \Gamma_1(\tau)\|_2 d\tau.$$

A technical complication is the appearance of the logarithmically singular Hankel function, which in this case can not be replaced by its expansion for large arguments as before in (5), where it led to a simpler oscillatory exponential. An alternative is to substitute the Hankel function by its Mehler-Sonine integral representation [16, (10.9.10)], which has a complex exponential in the integrand. After interchanging integration variables, a regular steepest descent analysis can be applied on the resulting bivariate integral [14].

The main observation to make here is that, in the absence of multiple scattering effects, the only contribution to the singular oscillatory integral originates in the singularity at  $\tau_1 = \tau$ . As one can apply a path of steepest descent such that the Mehler-Sonine integral representation of  $H_0^{(1)}$  does not contribute to the phase of the integrand, the phase of  $S_{11}V_1$  indeed equals the phase of  $V_1$ .

In order not to change the shape of our mode (3) after another reflection, the phase on  $\Gamma_1$  should equal the phase of the integral (5) up to a constant shift  $\mu$ . This is expressed by the equation

$$\phi(\tau_1) + \mu = \delta[\tau_1, \chi(\tau_1)] + \phi[\chi(\tau_1)]. \quad (7)$$

The phase shift  $\mu$  will correspond to half the phase of the eigenvalue, i.e. we have that  $\lambda = ce^{2ik\mu}$ . It must equal half the path length of the periodic orbit, and indeed  $\mu = d$  follows from (7) in the special case  $\tau_1 = \chi(\tau_1) = 0$  that corresponds to the shortest path.

## 5 Symbolic computation of Taylor coefficients of $\phi$

The system of equations that  $\phi(\tau)$  and  $\chi(\tau)$  should satisfy is (6)–(7). This is a non-linear system which even in the case of two circles does not seem to allow an explicit analytic solution. We resort to series expansions that do lead to fully explicit expressions for the coefficients.

We look for a Taylor series of the form

$$\phi(\tau) \sim \sum_{i=0}^{\infty} c_i \tau^i.$$

We are free to choose the constant  $c_0$ , since it corresponds purely to a constant phase shift and eigenfunctions are only determined up to a constant factor: we set  $c_0 = d$ . We expand the other relevant functions into Taylor series as well:

$$\begin{aligned} \chi(\tau_1) &\sim \sum_{j=0}^{\infty} a_j \tau_1^j \\ \phi[\chi(\tau_1)] + \delta[\tau_1, \chi(\tau_1)] - \phi(\tau_1) &\sim \sum_{i=0}^{\infty} \omega_i \tau_1^i \\ \left. \frac{\partial \delta[\tau_1, \tau_2] + \phi(\tau_2)}{\partial \tau_2} \right|_{\tau_2=\chi(\tau_1)} &\sim \sum_{i=0}^{\infty} \psi_i \tau_1^i \end{aligned}$$

We already know that  $a_0 = 0$  since  $\chi(0) = 0$ . Note that the coefficients  $\omega_i$  and  $\psi_i$  can be computed explicitly in terms of  $a_i$  and  $c_i$ , since we can explicitly expand the Euclidean distance function  $\delta[\tau_1, \tau_2]$  as well.

The coefficient  $\omega_0$  may be nonzero because of (7): it is equal to  $\mu = d$ . All other coefficients are computed in a recursive procedure: for each index  $i$ , starting from  $i = 0$ , we solve  $\omega_{i+1} = 0 = \psi_i$  for  $a_i$  and  $c_{i+1}$ . The newly found coefficients can be used in the next iteration.

For the case of the two circles,  $\omega_1 = 0 = \psi_0$  yields

$$a_1 c_1 - c_1 = 0 = c_1 \quad \Rightarrow \quad c_1 = 0,$$

which is intuitively correct due to symmetry. For  $i = 1$ , we obtain a system of quadratic equations

$$\begin{aligned} 0 &= \frac{3}{2}\pi^2 a_1^2 - \pi^2 a_1 + a_1^2 c_2 + 3/2\pi^2 - c_2, \\ 0 &= 3\pi^2 a_1 - \pi^2 + 2a_1 c_2 \end{aligned}$$

from which we deduce

$$c_2 = \sqrt{2}\pi^2, \quad a_1 = 3 - 2\sqrt{2}.$$

We have discarded the other solution  $a_1 = 3 + 2\sqrt{2}$ ,  $c_2 = -\sqrt{2}\pi^2$  as the left side of Figure 3 indicates that  $c_2 > 0$  and, furthermore,  $a_1 > 1$  would imply moving away from the periodic orbit shown in the left part of Figure 2. For higher  $i$ , the system of equations is linear in the coefficients and the solution is unambiguous. Due to symmetry, all  $a_i = 0 = c_{i+1}$  for even  $i$ .

Further computation leads to the next nonzero coefficients

$$c_4 = \frac{-11}{12}\sqrt{2}\pi^4, \quad a_3 = 7\pi^2(17\sqrt{2} - 24)$$

and

$$\begin{aligned} c_6 &= \frac{2783\sqrt{2}\pi^6}{2520}, & a_5 &= \frac{\pi^4}{84}(1205811\sqrt{2} - 1705312), \\ c_8 &= \frac{-358021}{205632}\sqrt{2}\pi^8, & a_7 &= \frac{-\pi^6}{128520}(289615597399\sqrt{2} - 409578202752). \end{aligned}$$

## 6 A geometric interpretation

We can assign a geometric meaning to the stationary point function  $\chi(\tau)$ . Recall that  $\chi(\tau_1)$  is the point on  $\Gamma_2$  from which a ray hits the point  $\Gamma_1(\tau_1)$ . By symmetry, the converse also holds, and applying  $\chi$  again yields a point back on  $\Gamma_1$ . In the sequence  $\chi(\chi(\tau_1))$ ,  $\chi(\tau_1)$ ,  $\tau_1$ , it should be true that the incoming and reflected ray at the middle point  $\chi(\tau_1)$  on  $\Gamma_2$  are at equal angles with the normal direction. In our setting, this leads to the equation

$$\begin{aligned} 0 &= 4\pi\chi(\tau_1) + \arctan\left(\frac{r \sin(2\pi\chi(\tau_1)) - r \sin(2\pi\chi[\chi(\tau_1)])}{d + 2r - r \cos(2\pi\chi(\tau_1)) - r \cos(2\pi\chi[\chi(\tau_1)])}\right) \\ &\quad + \arctan\left(\frac{r \sin(2\pi\chi(\tau_1)) - r \sin(2\pi\tau_1)}{d + 2r - r \cos(2\pi\chi(\tau_1)) - r \cos(2\pi\tau_1)}\right). \end{aligned} \tag{8}$$

This equation is again highly non-linear, and is hard to get a symbolic solution on account of the application of  $\chi$  on itself. Therefore, one computes a Taylor series of this expression for  $\tau_1$  near zero, sets all coefficients equal to zero and this results in the same  $a_i$  as in the procedure described before.

One can numerically approximate  $\chi$  using (8), and can then obtain the phase in a limited range of  $\tau$  via (6):

$$\phi(\tau) = - \left( \int \frac{\partial \delta(\tau_1, \tau_2)}{\partial \tau_2} \Big|_{\tau_2=\chi(\tau_1)} \chi'(\tau_1) d\tau_1 \right) \Big|_{\tau_1=\chi^{-1}(\tau)}. \tag{9}$$

To obtain  $\phi$  in a wider domain, one notes that the phase is defined in terms of itself and the distance to a stationary point on the other obstacle, as equation (7) expresses. It is this self-referential definition of the limiting phase that complicates an analytical expression. However, one can note that phases in high-frequency wave scattering correspond to the length of the trajectory of a ray. In a homogeneous medium, rays are straight lines and phases correspond to distances. Our rays originate in a small region around the periodic orbit and reflect outward until they leave the scene, but it is easier to think of them travelling in the opposite way. The length of such a path, followed by recursive application of  $\chi$ , is infinite because of the infinite number of reflections. However, we already take into account a phase shift  $\mu$  at each reflection in the eigenvalue  $\lambda$ . So, writing  $\chi^{[r]}$  for the function  $\chi$  applied  $r$  times to the identity, a geometrical interpretation of the phase is

$$\phi(\tau) = c_0 + \sum_{r=0}^{\infty} \left( \delta(\chi^{[r]}(\tau), \chi^{[r+1]}(\tau)) - \mu \right). \quad (10)$$

## 7 Results

We first compute  $\chi$  by applying six functional Newton iterations on (8) with an initial guess  $\chi(\tau) \approx (3 - 2\sqrt{2})\tau$  in Chebfun [19]. This satisfies (8) up to machine precision and its series expansion coefficients also correspond to our  $a_i$ . We have added a few iterations of  $\chi$  as dashed purple lines in Figure 2: the ray is nearly indistinguishable from the periodic orbit after the second reflection. Next, we compute the phase as (10) where we choose  $c_0 = 1$  and we end the summation after  $r = 10$  reflections as the next term is near machine precision. The series expansion coefficients of this phase also converge to our  $c_i$ , and  $\phi(\tau)$  is not equal to  $\delta[\tau, \chi(\tau)]$ .

In Figure 3, one can see that this phase lies in between the two physical distances  $\zeta$  and  $\xi$  shown in Figure 2. These are the distances from a point on  $\Gamma_1$  to the point  $\Gamma_2(0)$  or to the closest point on the other circle respectively. These physical distances may be suitable starting points for an iterative procedure to solve the non-linear system of equations (6)–(7) in a more general setting. In the right part of Figure 3, we also see that our Taylor expansions with coefficients  $c_i$  converge with the expected orders. The phase can indeed also be computed as (9), although in a smaller domain due to the inverse of  $\chi$ .

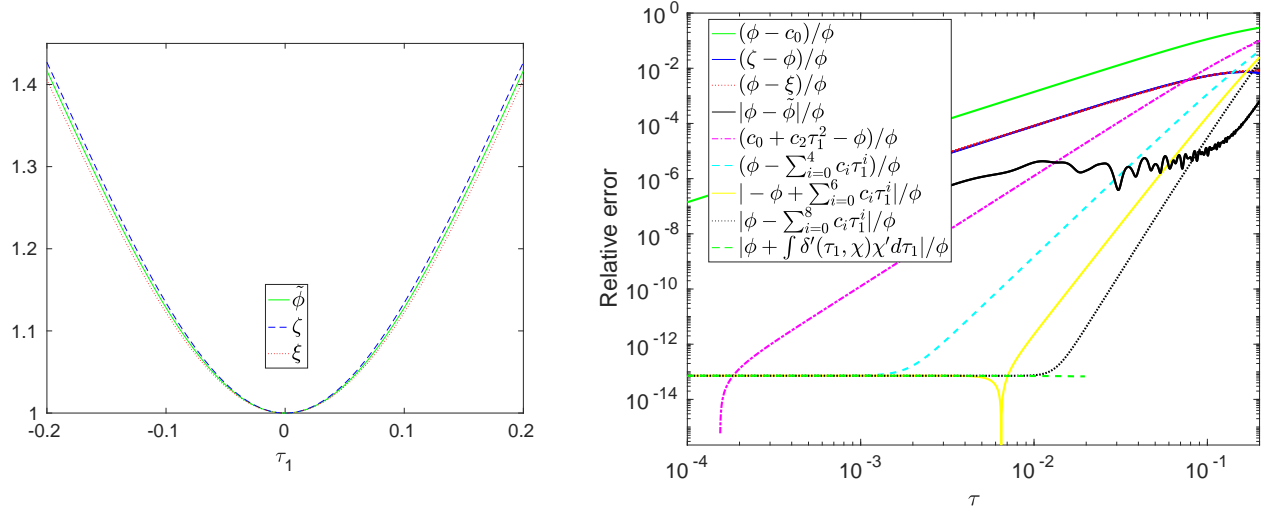


**Figure 3:** Distances and phase  $\phi(\tau)$  from (10) (left) and relative errors with respect to the latter for the former, our symbolical series expansion,  $\tilde{\phi}$  and (9) (right).

In order to show that these solutions are indeed related to an eigenvalue problem, we discretized the scattering problem in a classical boundary element method. The radius  $r = 1/2$ , the wavenumber  $k = 2^9$

and the number of degrees of freedom  $N = 10k$  in a collocation scheme with piecewise linears. We computed the eigenvalue decomposition of the matrix  $M$  and selected the eigenvector  $V_{j,1}$  corresponding to the largest eigenvalue, see Figure 2.

From this vector, we compute an approximate phase  $\tilde{\phi}(\tau)$  as follows. We have chosen  $\phi(0) = d$ , half the length of the periodic orbit. Assuming that the argument of  $v_{\text{smooth}}(\tau)$  varies much more slowly than  $\text{Arg}(\exp[ik\phi(\tau)])$ , the estimated reference phase  $\tilde{\phi}$  at other collocation points  $\tau_{1,j}$  is:

$$\tilde{\phi}(\tau_{1,j}) = \tilde{\phi}(\tau_{1,j\mp 1}) + \frac{\text{Arg}(V_{j,1}) - \text{Arg}(V_{j\mp 1,1})}{k} - \frac{2\pi}{k} \left\lfloor \frac{\text{Arg}(V_{j,1}) - \text{Arg}(V_{j\mp 1,1})}{2\pi} \right\rfloor.$$

In the right part of Figure 3, the error of  $\tilde{\phi}$  is about  $10^{-6}$  due to the accuracy of  $V_{j,1}$  with respect to the continuous problem and because we compute its angles. We have also been able to verify that the coefficients of polynomial approximations of  $\tilde{\phi}(\tau_1)$  converge to the respective  $c_i$ .

## 8 Conclusions

At high frequencies, standard boundary element methods become computationally too expensive, while the cost of hybrid numerical-asymptotic methods can be frequency-independent. However, these require a priori information on the phase of the solution, for example via ray tracing. We note that this phase converges to some equilibrium after a number of reflections in a multiple scattering scene, and it is given by the phase of the eigenfunction of the operator representing a full cycle of reflections.

For the case of two circles, we can find all coefficients in the Taylor expansion of the phase  $\phi(\tau_1)$  via a simple and recursive scheme. This phase is given by the distance to the periodic orbit via an infinite number of reflections, where one subtracts the distance between the circles at each reflection.

The scheme to compute the Taylor coefficients is not dependent on the wavenumber nor on the incident wave, an advantage when computing the ‘Radar cross section’ for example. In the future, we intend to find a series expansion of  $v_{\text{smooth}}(\tau)$  as well. Though the computations in this paper were specific to the case of two circles, we also expect a similar methodology to work for arbitrary collections of more general objects.

## Acknowledgments

The authors would like to thank Samuel Groth and Marcus Webb for interesting and useful discussions on topics related to this paper. The authors were supported by FWO Flanders [projects G.0617.10, G.0641.11 and G.A004.14].

## References

- [1] T. ABOUD, J.-C. NÉDÉLEC, AND B. ZHOU, *Méthode des équations intégrales pour les hautes fréquences*, CR Acad. Sci. I Math., 318 (1994), 165–170.
- [2] A. Anand, Y. Boubendir, F. Ecevit, and F. Reitich. Analysis of multiple scattering iterations for high-frequency scattering problems. II: The three-dimensional scalar case. *Numer. Math.*, 114:373–427, 2010.
- [3] A. Asheim and D. Huybrechs. Local solutions to high-frequency 2D scattering problems. *J. Comput. Phys.*, 229:5357–5372, 2010.
- [4] A. Asheim and D. Huybrechs. Extraction of uniformly accurate phase functions across smooth shadow boundaries in high frequency scattering problems. *SIAM J. Appl. Math.*, 74(2):454–476, 2014.
- [5] V. M. Babich and V. S. Buldyrev. *Short-wavelength diffraction theory*. Springer-Verlag, Berlin, 1991.
- [6] N. Bleistein and R. A. Handelsman. *Asymptotic expansions of integrals*. Dover Publications, Inc., 31 East 2nd Street, Mineola, N.Y., 1986.

- [7] O. Bruno, C. Geuzaine, J. J. Monro, and F. Reitich. Prescribed error tolerances within fixed computational times for scattering problems of arbitrarily high frequency: the convex case. *Phil. Trans. R. Soc. Lond. A*, 362:629–645, 2004.
- [8] Chandler-Wilde, I. S., Graham, S. Langdon, and E. Spence. Numerical-asymptotic boundary integral methods in high-frequency acoustic scattering. *Acta Numer.*, pages 89–305, 2012.
- [9] S. N. Chandler-Wilde, D. P. Hewett, S. Langdon, and A. Twigger. A high frequency boundary element method for scattering by a class of nonconvex obstacles. *Numerische Mathematik*, 129(4):647–689, 2015.
- [10] D. L. Colton and R. Kress. *Integral equation methods in scattering theory*. John Wiley & Sons, New York (N.Y.), 1983.
- [11] F. Ecevit and F. Reitich. Analysis of multiple scattering iterations for high-frequency scattering problems. I: The two-dimensional case. *Numer. Math.*, 114:271–354, 2009.
- [12] C. Geuzaine, O. Bruno, and F. Reitich. On the  $O(1)$  solution of multiple-scattering problems. *IEEE Trans. Magn.*, 41(5):1488–1491, 2005.
- [13] S. P. Groth, D. P. Hewett, and S. Langdon. Hybrid numerical-asymptotic approximation for high-frequency scattering by penetrable convex polygons. *IMA J. Appl. Math.*, 80:324–353, 2015.
- [14] S. P. Groth, D. Huybrechs and P. Opsomer. High-order terms in the ray expansion for high-frequency scattering by single and multiple obstacles. 2017. In preparation.
- [15] D. Huybrechs and S. Vandewalle. On the evaluation of highly oscillatory integrals by analytic continuation. *SIAM J. Numer. Anal.*, 44(3):1026–1048, 2006.
- [16] NIST. NIST Digital Library of Mathematical Functions. <http://dlmf.nist.gov/>, 2016. Online companion to [17].
- [17] F. W. J. OLVER AND D. W. LOZIER AND R. F. BOISVERT AND C. W. CLARK, *NIST Handbook of Mathematical Functions*, Cambridge University Press, New York, 2010, Print companion to [16].
- [18] P. Opsomer. <https://github.com/popsomer/asyBEM/releases>, March 2017. Release 1: Coupling modes in two circles.
- [19] The University of Oxford & the Chebfun Developers. Chebfun, <http://www.chebfun.org/>, 2017.
- [20] R. S. Wong. *Asymptotic approximations of integrals*. SIAM, 3600 Market Street, 6th floor, Philadelphia (Pa.) 19104-2688 USA, 2001. Republication of 1944.
- [21] T. Wu. *Boundary element acoustics*. WIT Press, 2000. Reprint 2005.